15TH IEA HEAT PUMP CONFERENCE
MAY 26–29, 2026 | HOFBURG
VIENNA 2026
DECARBONISATION THROUGH INNOVATION

Performance Enhancement of Small-Scale Heat Pumps Using Thermoelectric Active Subcooling: A Simulation-Based Assessment

Jerik Catal, Mustafa Kalfa, Michael Lauermann, Fabrizia Giordano, Stephan Kling, Christian Köfinger, and Ahmed A. Serageldin *

Sustainable Thermal Energy Systems, Center for Energy, AIT Austrian Institute of Technology GmbH, 1210 Vienna, Austria

Abstract

Achieving climate-neutral buildings requires compact and efficient heating technologies suitable for small-scale residential applications. This study evaluates the integration of thermoelectric (TE) modules as an active subcooler in a 5 kW air-to-water heat pump (HP) and compares its performance with a conventional passive subcooler and reference HP. An equation-based model of the TE module under constant-voltage operation is developed, validated, and coupled with the heat pump to simulate multiple operating scenarios combining different heat sources (-12 °C, and 12 °C), sink temperatures (35 °C, and 65 °C), and refrigerants (R290, R1234zee, and R1234yf).

Results show that TE-assisted subcooling consistently contributes to the total heating capacity (5 kW) by 10–17%, with contribution of 0.54–0.96 kW. Highest COP improvements of up to 13% are achieved under high-lift heating conditions (65 °C Radiator/DHW, dT: 15K), while lower-temperature floor-heating (35 °C Floor Heating dT:5 K) conditions yield capacity gains but minimal efficiency improvement. Despite the added TE electrical input of 0.09–0.11 kW, the active system consumes less total power than the passive subcooler configuration due to reduced compressor work which reaches to more than 20% saving of electrical energy consumption.

The findings demonstrate that active TE subcooling provides clear advantages over passive subcooling and offers the benefits under high-lift operation compared to reference HP. Overall, TE integration is shown to be a promising and technically viable approach for enhancing the efficiency of next-generation small-scale heat pumps in residential and urban heating applications.

Future work should examine the impact of TE coupling position within the refrigeration circuit, as placement may influence subcooling effectiveness and system-level performance. Additionally, a comprehensive economic and techno-economic assessment is recommended, particularly for scaling TE integration to medium and large heat pump systems exceeding 50 kW, where cost-performance trade-offs become increasingly critical.

Keywords: Thermoelectric subcooling; Active subcooler, Low-GWP refrigerants

1. Introduction

The building sector is responsible for 30% of the global final energy consumption and 26% of global energy-related emissions [1]. This poses the urgent need for sustainable and innovative approaches to decarbonize the residential sector, particularly in heating, cooling, and ventilation. Heat pumps (HPs) are a well-established technology which help fulfilling this scope, by efficiently transferring heat from low-temperature sources to higher temperature sinks using electricity. In particular, air-source heat pumps (ASHPs) represent a mature

* Corresponding author. Tel.: +
E-mail address: ahmed.serageldin@ait.ac.at

solution for building decarbonization, providing both heating and cooling services to buildings with high coefficients of performance, simple installation and lower investment costs compared to other HPs [2]. However, its widespread adoption still faces several technical, economic, social and safety challenges. From a technical perspective, their efficiency strongly depends on the available source and sink temperatures. For instance, when operating in cold climate regions, conventional ASHPs experience multiple performance limitations, such as high discharge temperatures and compression ratios [3], decreased heating capacity and efficiency [4], as well as loss of performance due to frost formation [5]. From an economic standpoint, the deployment of large-scale ASHPs may be hindered by the relatively high initial investment cost, combined with high operational expenditures coming from unfavourable electricity-to-gas price ratios [6], especially in regions with limited financial incentives. In addition, their mechanical complexity and characteristics generate vibration and acoustic noise during operation, often exacerbated by frosting [7], which can lower user comfort and social acceptance [8]. Safety risks associated with the choice of refrigerants also contribute to resistance to their public acceptance, following the adoption of highly flammable natural refrigerants in response to progressively stricter EU regulations on global warming potential (GWP) mitigation [9]. Therefore, it is of clear importance to investigate innovative solutions capable of overcoming or compensating for the limitations of conventional HPs, thus facilitating their broader integration into the market.

Within this context, thermoelectric (TE) modules emerge as a promising alternative that satisfies several environmental, technical, and economic requirements. A TE module is a solid-state energy converter composed of multiple thermocouples connected electrically in series and thermally in parallel [10]. Each thermocouple is made of two semiconductor elements, n-type and p-type, joined together using copper tabs and sandwiched between ceramic plates, which generate a thermoelectric heating or cooling effect (also known as Peltier effect) when subjected to an electric current. This enables the TE device to function as a solid-state heat pump for heating and cooling applications, without the use of any oil, refrigerants or moving parts [11]. Conversely, when a temperature difference is applied across the junctions of two different types of wire, a voltage difference is generated, ultimately leading to the flow of electrical current [12]. This effect (also known as Seebeck effect) constitutes the working principles of thermoelectric generators (TEGs), which convert waste heat into electrical energy.

The selection of the semiconductor material plays a crucial role in the efficiency of the TE module. Specifically, the figure of merit (ZT) of TE materials depends on factors such as the Seebeck coefficient, electrical and thermal conductivity of the material, and temperature. To achieve an efficiency comparable to current vapor compression-based heat pumps, TE materials need a ZT value close to 4 [13]. However, commonly used semiconductor materials, such as bismuth telluride ($\mathrm{Bi_2Te_3}$), lead telluride (PbTe), and silicon germanium (SiGe), typically exhibit ZT values ranging from 0.6 to 1.1 [14]. This severely impacts the conversion efficiency of the module, representing one of the major challenges towards broader implementation of the technology at the market level, together with its expensive production process. Particularly, the TE material represents 50-80% cost of the total TEG cost, which in the case of $\mathrm{Bi_2Te_3}$ is of around 115 $/kg [15]. Moreover, the cost is highly dependent on the number of TE modules in place. Shi et al. proposed an economic analysis on air-cooling application using different numbers of Peltier modules [16]. The authors concluded that, due to economies of scale, increasing the number of thermoelectric modules initially reduces the cooling cost (expressed as cost per unit of cooling). However, beyond a certain threshold, additional modules no longer provide economic benefit, and the investment becomes less profitable. Thus, economic profitability of TE modules becomes more predominant in smaller and compact systems, which demand flexible operation, without moving parts and low noise [17].

For direct integration in HP applications, TE modules are found particularly promising when integrated as subcoolers into vapor-compression systems. Several studies in literature confirm a notable increase in COP of above 20% for transcritical CO_2 ASHP [18,19], as well as increased capacity [20]. However, fewer studies have explored the use of TE modules for subcooling in systems operating with other types of refrigerants. Okuma et al. experimentally investigated the integration of a TE module within a vapor-compression cycle (VCC), as an intermediate third stage of an otherwise two-stage heat pump with R-410A [11]. They found that the system could achieve additional capacity (up to +48%) with comparable COP as in the base-case, at an ambient temperature of -17.8°C. Wantha conducted an experimental study of a thermoelectric subcooler within a R134a refrigerant system [21]. He found that, despite an increase in the COP of ca. 27%, the high power consumption of the module during operation led to a significant reduction in the potential COP of the system.

The novelty of this study lies in the application of thermoelectric (TE) modules as an active subcooling device within a small-scale (5 kW) air-to-water heat pump, offering a new approach to improving system efficiency without major design modifications. Unlike previous research focusing on large-scale or theoretical concepts, this work provides a comprehensive, scenario-based comparison between an active TE subcooler and a conventional passive subcooler under varying source, sink temperatures and refrigrants. The main objectives are to (1) evaluate the impact of TE-assisted subcooling on heat pump performance, particularly the coefficient of performance (COP); and (2) identify optimal operating conditions that balance performance improvement and energy consumption. Together, these aims contribute to advancing compact, high-efficiency heat pumps suitable for residential and urban heating applications.

2. TE-HP coupling models

In this study, a small-scale vapor-compression heat pump with a heating capacity of 5 kW is modeled using Dymola/Modelica. The system consists of four main components—compressor, condenser, expansion valve, and evaporator—arranged in a closed refrigeration loop, as illustrated in Fig. 1. This configuration serves as the reference model for subsequent comparisons. In the cycle, the refrigerant vapor exits the evaporator at state 1 and is compressed by the compressor to a high-pressure & high-temperature state (state 2). The refrigerant then flows into the condenser, where it releases heat to the sink fluid through a secondary water circuit that transfers the thermal energy to the building's heating system. As a result, the refrigerant condenses into a liquid at state 3, and subsequently expands through the expansion valve to state 4, completing the cycle.

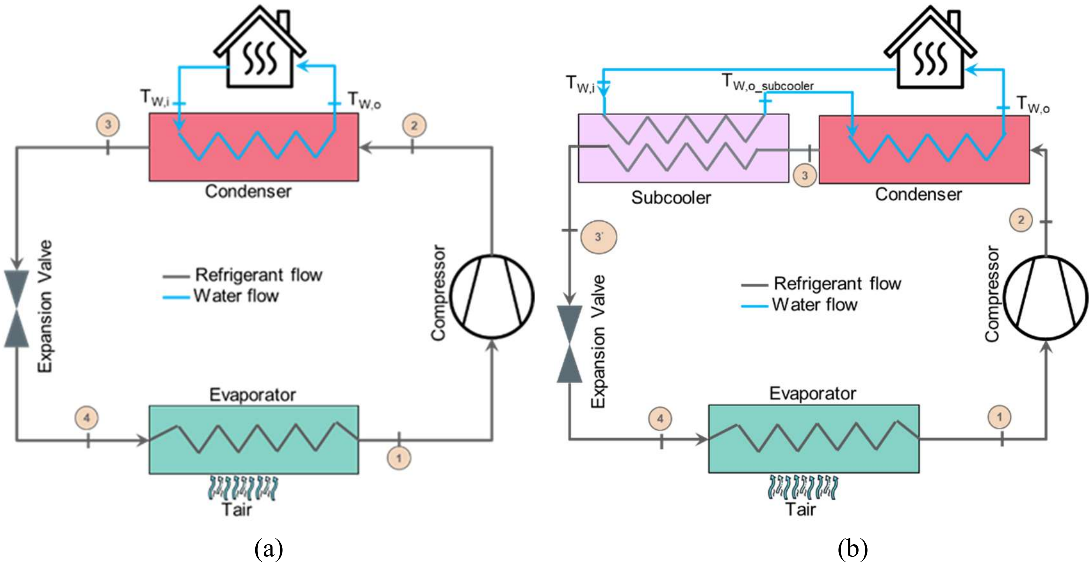

Fig. 1 Vapor-compression heat pump cycle a) Reference model, b) HP with a passive subcooler

According to the literature to use a simple and energy-efficient method to enhance heat pump performance without requiring external power input, the second reference model is proposed as depicted in Fig. (1b). In this configuration, a passive heat exchanger is integrated after the condenser to function as a subcooler, improving the thermodynamic efficiency of the vapor-compression heat pump. The subcooler enhances the degree of liquid subcooling before the expansion valve, thereby increasing the refrigerating effect and overall system coefficient of performance (COP). As illustrated in Fig. 1b, the refrigerant leaving the condenser at state 3 transfers part of its heat to the secondary (sink) fluid flowing toward the condenser through the passive subcooler. This internal heat exchange cools the liquid refrigerant to state 3′. The subcooled liquid then expands through the expansion valve to state 4, completing the cycle. Figure 2a illustrates the schematic of the vapor-compression heat pump equipped with an active thermoelectric (TE) subcooler. In this configuration, the cold side of the TE modules is thermally coupled to the refrigerant line after the condenser (state 3), providing additional cooling to the liquid refrigerant before it expands through the valve to state 3′. A total of ten TE modules are placed in series along the refrigerant line, ensuring progressive subcooling of the liquid refrigerant. Each module is independently powered by a constant voltage supply of 5 V, and its electrical input is individually calculated to assess performance. The hot side of the TE modules is exposed to the ambient environment, allowing heat rejection directly to the surroundings. The overall coefficient of performance (COP) of the system is determined by accounting for both the enhanced subcooling effect and the additional electrical power consumption of the TE modules. This configuration is hereafter referred to as the Single-Sided TE-HP model, representing the baseline active subcooling setup for subsequent analysis and comparison.

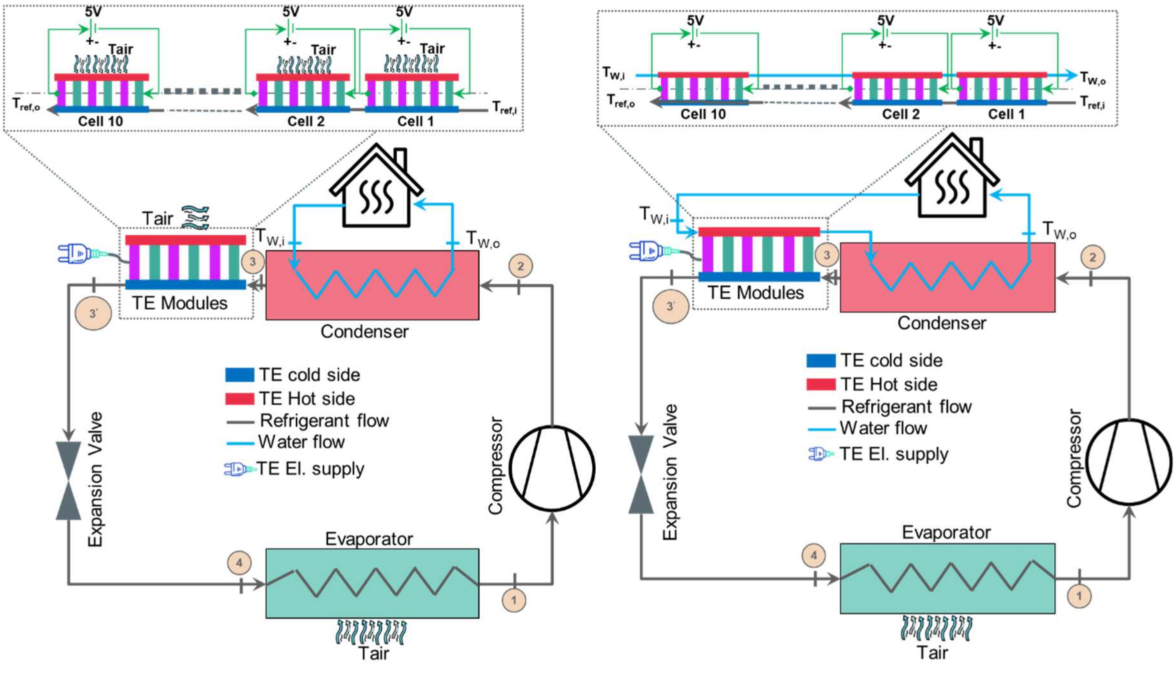

Fig. (2) Schematic representation of the vapor-compression heat pump with a) single sided TE modules (Single-Sided TE-HP model), b) double sided TE modules (Double-Sided TE-HP model)

Finally, Figure 2b depicted the schematic of the vapor-compression heat pump integrated with a dual-sided thermoelectric (TE) subcooler. In this configuration, the cold side of the TE modules is coupled to the refrigerant line downstream of the condenser (state 3) to provide additional subcooling before expansion at state 3′, while the hot side transfers heat to the secondary (sink) fluid flowing toward the condenser. This preheating process increases the inlet temperature of the refrigerant at the condenser inlet, thereby enhancing the overall heating capacity, defined as the combined heat output from both the condenser and the TE modules. This configuration is referred to as Double-Sided TE-HP model, designed to maximize heat recovery and system performance.

3. Lumped model of TE module

To simulate the thermal and electrical behaviour of the thermoelectric (TE) module, an equation-based model was developed to represent a constant-voltage-driven TE module. The applied voltage is fixed at 5 V, while the electrical current (I) and the resulting temperature difference (ΔT) across the module are determined dynamically until thermal and electrical equilibrium is achieved. Where (ΔT) is the temperature differences between hot ($\boldsymbol{T_h}$)and cold sides ($\boldsymbol{T_c}$) of TE module is expressed according to Eq. (1).

$$\boldsymbol{\Delta T = T_h - T_c} \qquad \textbf{(1)}$$

The electrical current through the TE module is calculated using given voltage (V), Seebeck coefficient (α) and electrical resistance (R) as shown in Eq. (2).

$$I = \frac{V-\alpha\ .\ \Delta T}{R} \qquad \textbf{(2)}$$

The corresponding electrical power input is then obtained as shown in Eq. (3)

$$P = I\,.V \qquad (3)$$

The cooling capacity (Q_c) on the cold side of the module is determined from the combined effects of the Peltier, Joule, and Fourier heat transfer terms:

$$Q_c = \alpha\,.I.T_c - 0.5\,I^2.R - K.\Delta T \qquad (4)$$

Where *K* is the thermal conductance of the TE module (W/K). Heating capacity (Q_h) is calculated using Eq. (5).

$$Q_h = Q_c + P \tag{5}$$

For known inlet temperatures, mass flow rates, and heat capacities of the hot and cold streams, ($T_{h,i}$, $\dot{m}_h$, Cp_h $T_{c,i}$, $\dot{m}_c$, Cp_c), the outlet temperatures of both sides can be calculated by Eqs. (6,7)

$$T_{h,o} = T_{h,i} - \frac{Q_c}{\dot{m}_h . Cp_h} \tag{6}$$

$$T_{c,o} = T_{c,i} + \frac{Q_h}{\dot{m}_c . Cp_c} \tag{7}$$

Assuming a perfect thermal contact with zero thermal resistance (*Rh*=*Rc*=0), the surface temperatures of the TE modules are equal to the corresponding bulk fluid temperatures. In the case of the Single-Sided TE-HP model, the hot side of the TE modules is maintained at the ambient temperature $T_{amb.}$

4. Dymola model of the HP with TE modules

A single-stage vapor compression heat pump is modelled in Dymola by using TIL library. It uses a working refrigerant and water/glycol mixtures on the secondary sides for the heat source and sink. The model follows the classical refrigeration cycle structure as explain in Fig. (1). Each component is modelled with energy, mass, and momentum conservation equations embedded in the TIL components framework. Evaporator and Condenser are implemented as NTU Type VLELiquidEvaporator and VLELiquidCondenser, connected to secondary loops with boundary conditions and controllers to maintain superheating/subcooling temperatures while compressor is modelled as variable efficiency vapor compression unit with electrical efficiency of η_el = 0.98. Multiple temperature and mass flow sensors, pressure sensors, and state point viewers are integrated for real-time observation of thermodynamic conditions across the cycle via log(p)-h diagram. In addition, the COPs are calculated as indicated in Eqs (8).

$$COP_h = \frac{Q_{cond.}}{P},\ COP_c = \frac{Q_{evap}}{P} \tag{8}$$

Then the TE modules series are integrated in the refrigeration circuit of the HP after condenser for subcooling purposes under both Single-Sided and Double-Sided configurations as depicted in Fig. (3). The integrated system performance coefficients are calculated using Eq.(9)

$$COP_h = \frac{Q_{cond.+} \sum_1^{10} Q_{h,TE}}{P + \sum_1^{10} P_{TE}},\ COP_c = \frac{Q_{evap}\ \sum_1^{10} Q_{c,TE}}{P + \sum_1^{10} P_{TE}} \tag{9}$$

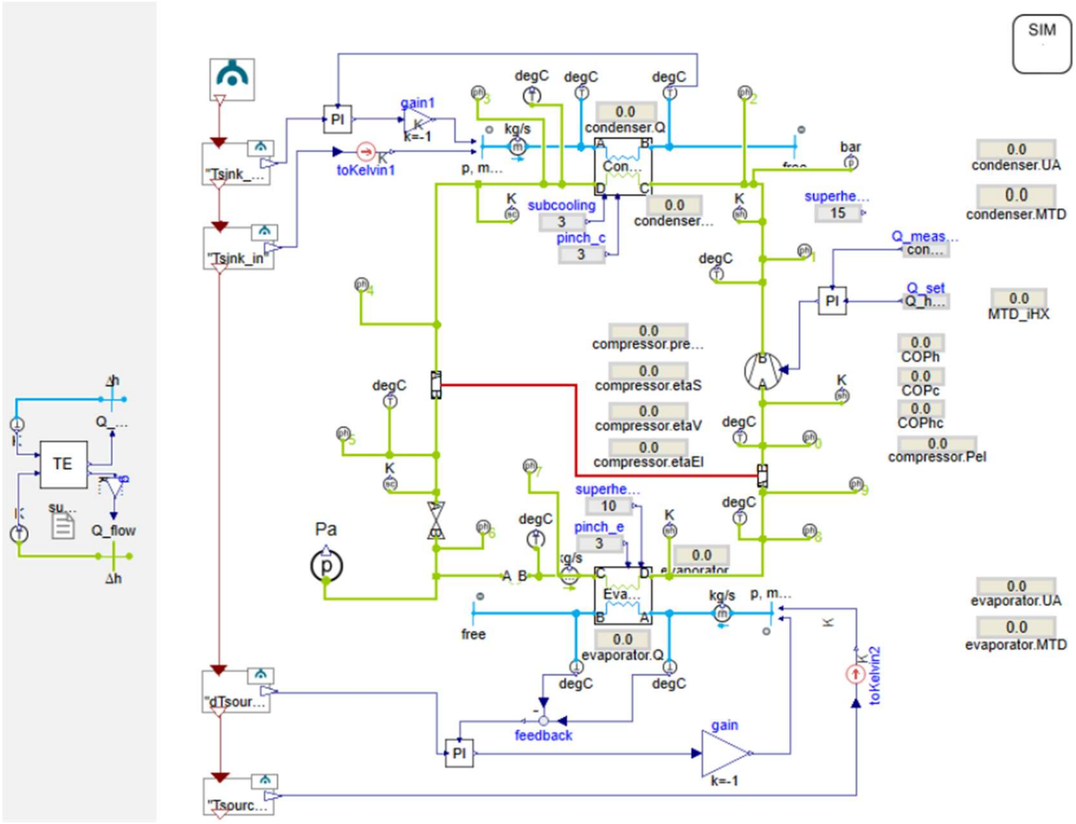

Fig. (3) Dymola model of the HP with Double-Sided TE modules

5. Validation of the Dymola Model

The TE model developed within TIL library was first validated with experimental measurements under the operating conditions listed in Table 1. Since the available experimental data corresponds only to the single-sided configuration, a Python-based model was developed using the same modelling approach to serve as an intermediate validation step between the experimental results and Dymola simulations. This additional step was necessary because experimental measurements for the Double-Sided configuration are not yet available. The validation process was performed by conducting a cell-by-cell comparison of the TE module parameters, including the cold-side temperature, hot-side temperature, heating capacity (Q_h), cooling capacity (Q_c), heating and cooling coefficients of performance (COP_h and COP_c), and electrical power consumption (P_{el}). The root means square error (RMSE) and mean absolute percentage error (MAPE) were then calculated for each variable to quantify the agreement between different models.

The validation results demonstrate strong agreement between the developed models and the measurement data. In the first validation stage, comparing the Python model with the experimental measurements performed by OTS, the maximum root mean square error (RMSE) and mean absolute percentage error (MAPE) were 0.189 W for the heat rejection (Q_h) and 0.55% for the temperature difference (ΔT), respectively. In the second validation stage, comparing the Dymola model with the Python model, the maximum RMSE and MAPE were 0.379 W for Q_h and 0.99% for ΔT. These low error values indicate a high level of consistency between simulation tools and experimental reference, confirming that the Dymola model accurately replicates the thermoelectric module’s thermal–electrical behavior. The overall validation accuracy of approximately 98% demonstrates the reliability of the developed Dymola TE model for subsequent integration into the heat pump system simulations

Table 1. List of Variables and Parameters used in Validation

<table>
<tr><th colspan="2"></th><th>Single Sided
TE Module</th><th>Double Sided
TE Module</th></tr>
<tr><td colspan="2">TE Cell parameters</td><td colspan="2">α = 0.122 V/K
R = 2.42 Ohm
K = 3.87 W/K</td></tr>
<tr><td colspan="2">Modules Chain</td><td colspan="2">N = 10,
Rc = 0 m.K/W
Rh = 0 m.K/W
V = 5 v</td></tr>
<tr><td rowspan="2">Flow fluids</td><td>Hot</td><td>Air</td><td>R290</td></tr>
<tr><td>Cold</td><td>R32</td><td>Water</td></tr>
<tr><td rowspan="2">Flowing fluids cond.</td><td>Hot</td><td>35°C</td><td>Th = variable depends on BC
Q = 0.08 kg/s</td></tr>
<tr><td>Cold</td><td>Tc = 35°C,
Q =0.0229 kg/s</td><td>Tc = variable depends on BC
Q = 0.012 kg/s</td></tr>
<tr><td colspan="2">Validation</td><td>Exp. VS Python VS Dymola</td><td>Python Vs Dymola</td></tr>
</table>

6. Simulation Scenarios

After validating the Dymola model with the coupling of double-sided TE modules following the methodology described in the previous section, multiple simulation scenarios were conducted to determine the optimal coupling arrangement of the system under varying source and sink temperature conditions and for different refrigerants. The increase in total heating capacity and the improvement in the heating coefficient of performance (COP_h) were selected as the primary key performance indicators (KPIs) for evaluating system performance. All performance improvements are evaluated relative to the Reference Heat Pump model (Model 0). A broad set of simulations was conducted to explore various TE–HP coupling configurations for subcooling enhancement, after which the scenario space was systematically filtered to focus on the most promising coupling positions and performance outcomes. Then, the complete list of simulated scenarios and their corresponding operating and boundary conditions is provided in Table 2.

The simulation matrix includes two heat sources—air at −12 °C representing cold-climate ambient conditions, and wastewater at 12 °C representing a mild, stable renewable heat source. Two sink supply temperature levels were considered: 65 °C for radiator-based systems (typical in retrofitted buildings) and 35 °C for low-temperature floor heating systems, common in modern energy-efficient buildings. To examine the influence of refrigerant thermophysical properties, three low-GWP refrigerants—R290, R1234yf, and R1234zee—were investigated. These refrigerants were chosen for their environmental compatibility, favourable thermodynamic performance, and potential applicability in future heat pump systems under forthcoming F-gas regulations. In each simulation scenarios, a comprehensive analysis was performed in order to evaluate both the thermoelectric (TE) module performance and the overall TE–heat pump (TE-HP) coupling performance. The key TE module performance indicators include the cold-side temperature, hot-side temperature, heating capacity (Q_h), heating coefficient of performance (COP_h), and electrical power consumption (P_{el}). For the TE-HP coupling, the primary performance indicators include the total heating capacity (Q_h), electrical input power (P_{el}), and the overall system heating coefficient of performance (COP_h). Additionally, the percentage increase and improvement in both Q_h and COP_h are calculated relative to the Reference Heat Pump model to quantify the benefits of integrating the TE modules under different operating conditions. In each scenario, three models were simulated, namely Reference HP model, HP with a passive subcooler, and HP with an active subcooler (TE modules).

Table 2 Simulation scenarios for the HP with Double Sided TE modules

Cases	Source		Sink (Supply to Heating system)		Refrigerant		
	Air -12 ºC	Wast Water 12 ºC	Radiator 65 ºC dT:15K	Floor heating 35 ºC dT: 5K	R290	R1234yf	R1234zee
1	√		√		√		
2		√	√		√		
3	√			√	√		
4		√		√	√		
5	√		√			√	
6	√		√				√
7	√			√		√	
8	√			√			√

7. Results and Discussion

7.1. Active vs Passive Subcoolers Under Various Source and Sink Temperatures

Figure 4 illustrates the distribution of heating capacity between the condenser and the TE modules for different sink/source temperatures with R290 and highlights the corresponding improvement in system COP relative to the reference heat pump. Across all operating conditions, the integration of TE modules leads to a consistent increase in total heating capacity, contributing between 0.54 and 0.87 kW of additional useful heat. This added heat represents a 10–17% enhancement over the baseline, demonstrating that the TE modules provide a significant supplementary heating effect independent of source and sink temperature. However, the extent to which this added heat translates into efficiency improvements depends strongly on the thermal boundary conditions. When operating with a high sink temperature (65 °C)—typical of radiator or DHW systems—the heat pump with TE modules exhibits clear COP gains. For the cold-air case (–12 °C), the COP improves by 12.6 %, while the mild-air case (12 °C) achieves the COP improvement of 11.5%, reflecting the favorable thermodynamic coupling when both the evaporator and the TE module operate under larger temperature differences. Under these conditions, the additional heating capacity provided by the TE modules become more than their electrical consumption, thereby improving overall system efficiency.

In contrast, when supplying heat at 35 °C (floor heating conditions), the system shows a COP improvement of 4.9 %, despite a meaningful increase in heating capacity. This outcome is expected because the reduced temperature lift on the sink side limits the effective temperature difference across the TE modules, lowering their thermodynamic leverage. As a result, the extra electrical input is balanced by the increase in delivered heat, leading to capacity enhancement but no efficiency gains.

On the other hand, the passive subcooler contribute maximally with 0.61 kW to heating capacity under a lifted sink temperature of 65 oC nd therefore delivers improvement in COP achieves maximum value of 8.1 %, functioning solely as a liquid-line heat exchanger that stabilizes refrigerant conditions without enhancing system output.

Figure 5 compares the total electrical power consumption of the heat pump system equipped with the active subcooler (TE modules) against the system using a passive subcooler across four operating scenarios. In every case, the active TE-HP configuration consumes less total electrical power than the passive configuration, despite the TE modules' own electrical demand. The TE modules draw only 0.09–0.10 kW, which is a small addition relative to the dominant heat pump compressor load. Nevertheless, the overall power consumption of the active system remains lower because the TE-induced subcooling reduces the compressor working ratio.

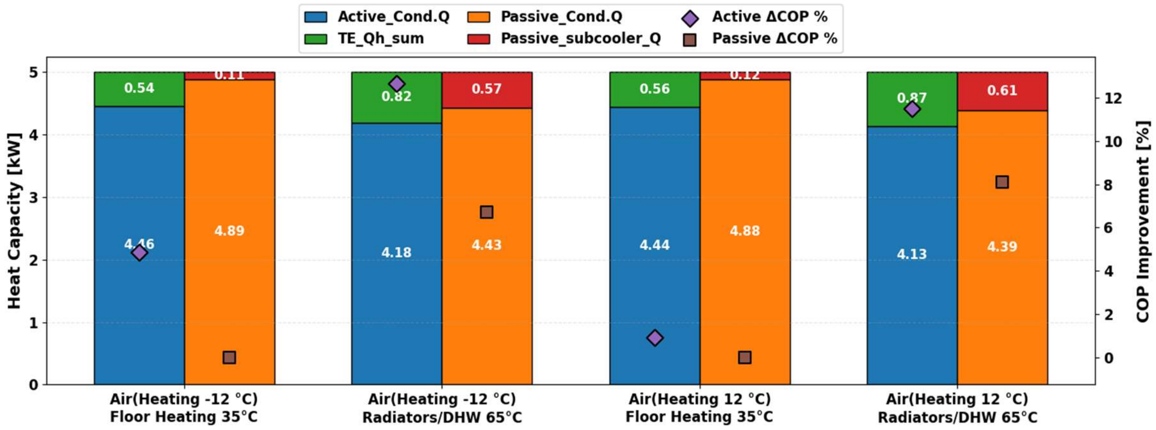

Fig. (4) Heating capacity distribution and COP improvement compared with reference model Fig. 1a for the HP with TE modules under four different operating conditions with refrigerant R290

Under the most challenging operating condition (source at –12 °C, sink at 65°C), the passive system requires 2.15 kW, whereas the active system requires only 1.70 kW, representing a substantial 21% reduction in electrical consumption. A similar trend is observed for the milder source temperature (12 °C) with the same sink, whereas the active configuration consumes 1.22 kW compared to 1.52 kW for the passive case, an improvement of roughly 20%. For floor heating at 35 °C, the absolute power demand is lower in both systems, but the active configuration still consistently outperforms the passive one, with the reduction of 14–20% depending on source temperature.

These results confirm that the active TE subcooler not only increases the heating capacity but also reduces the compressor working ratio, leading to a net reduction in total electrical power consumption.

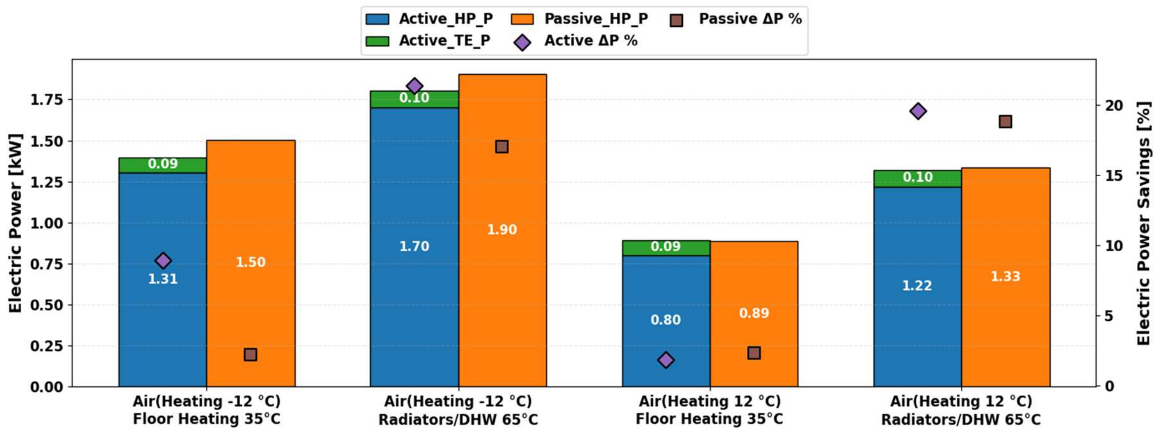

Fig. (5) Comparison of electrical power consumption between active (TE modules) and passive subcooler under four different operating conditions with refrigerant R290

As further elaboration and justification of the results presented in Fig. (4) and (5), Fig. (6a) and Fig. (6b) show the temperature profiles of both water and refrigerant flows passing through the active and passive subcoolers, respectively, under the operating conditions of a source at –12 °C and a sink at 65 °C. The figures clearly demonstrate the superior cooling capability of the active subcooler. The active configuration achieves a refrigerant temperature of 18.2 °C, compared to only 13 °C for the passive subcooler. The passive subcooler is inherently constrained by the thermodynamic energy balance between the hot and cold streams, which limits the maximum achievable temperature difference to approximately 16 °C. As a result, the passive subcooler cannot extract additional heat once the refrigerant and water streams approach to the thermal equilibrium.

In contrast, the active subcooler (TE modules) is not bound by this equilibrium limitation, as it can actively pump heat from the refrigerant to the hot side of the TE modules by using electrical input. This enables a larger temperature lift, deeper subcooling, and a more pronounced reduction in refrigerant temperature. The enhanced subcooling increases the refrigerant's enthalpy difference across the expansion valve, thereby improving the evaporator's effectiveness and contributing to the higher heating capacity and COP improvement observed in Fig. (5). These temperature profiles reinforce the fundamental advantage of active subcooling over passive subcooling, especially under high-lift operating conditions where deeper subcooling has the greatest impact on the system performance.

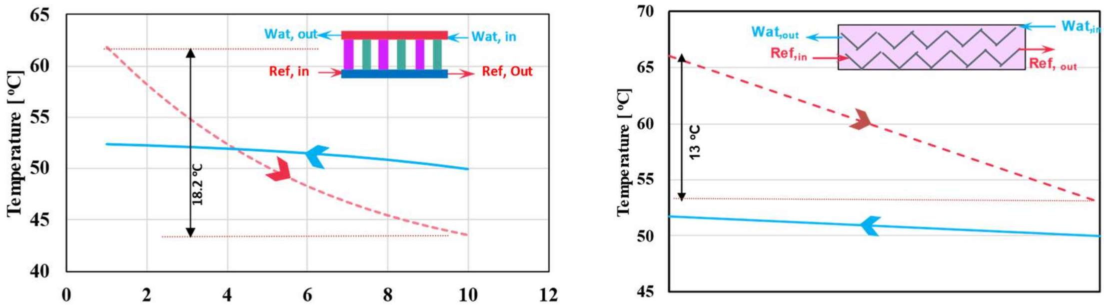

(a) (b)

Fig.(6) Temperature distribution of Water and Refrigrant, a) Active Subcooler, b) Passive Subcooler

7.2. Performance of an Active Subcooler with various Refrigerants

Figure (7a) compares the performance of the heat pump with TE modules for different low-GWP refrigerants (R1234yf, R1234zee, and R290) under two different sink temperatures of 35°C and 65°C and a source temperature of –12 °C, showing that TE integration consistently enhances heating capacity across all refrigerants, with contributions ranging from 0.54 to 0.96 kW. The largest TE heating contribution and highest efficiency gains occur with R1234yf, particularly at the 65 °C sink temperature, where COP improvements reach 17.5 %, followed by R1234zee and R290. This demonstrates that refrigerants with higher temperature lift across the condenser enable stronger synergy with the TE modules. At the sink temperature of 35 °C, TE modules still provide measurable extra capacity but yield minimal COP improvement (4–6%), as the reduced thermal gradient limits the TE effectiveness. Overall, the results highlight that the subcooling with TE modules is more beneficial in high-lift heating applications, and the R1234yf offers the strongest performance gains. Figure (7b) presents the electrical power consumption of the heat pump with TE modules. Across all scenarios, the TE modules consume only 0.09–0.11 kW, representing a small and nearly refrigerant-independent fraction of the total electrical consumption. At the sink temperature of 65 °C, the total power consumption is less than 1.744 kW, with only minor variation between refrigerants, indicating that the electrical demand of TE modules is largely unaffected by refrigerant types. Overall, the results demonstrate that refrigerant selection is a critical factor for heating capacity and COP, yet it exerts a negligible influence on the total power consumption of the heat pump. Further, a more in-depth investigation is required to fully assess refrigerant-dependent behaviour by comparing TE-assisted operation against a reference heat pump model operating with the same refrigerant.

8. Conclusions

This study evaluates the integration of thermoelectric (TE) modules as an active subcooler in a 5 kW vapor-compression heat pump under a wide range of operating conditions, type of refrigerants, and various source/sink temperature combinations. The conclusions are as follows:

1- Active subcooler (TE modules) consistently increases heating capacity, providing 0.54–0.96 kW of additional heat depending on type of refrigerant and boundary conditions. This corresponds to a 10–17% increase relative to the reference heat pump.
2- The performance enhancement achieves the most under high-lift heating conditions (65 °C sink), where the TE modules operate with a larger temperature difference.
3- In terms of electrical performance, the TE modules contribute only 0.09–0.11 kW of additional power consumption, representing a small, nearly refrigerant-independent overhead.
4- Despite this additional load, the overall electrical demand of the HP with active subcooler is consistently lower than that of the one with passive subcooler.
5- The system achieves COP improvements of 10–13%, with R1234yf showing the highest gains.

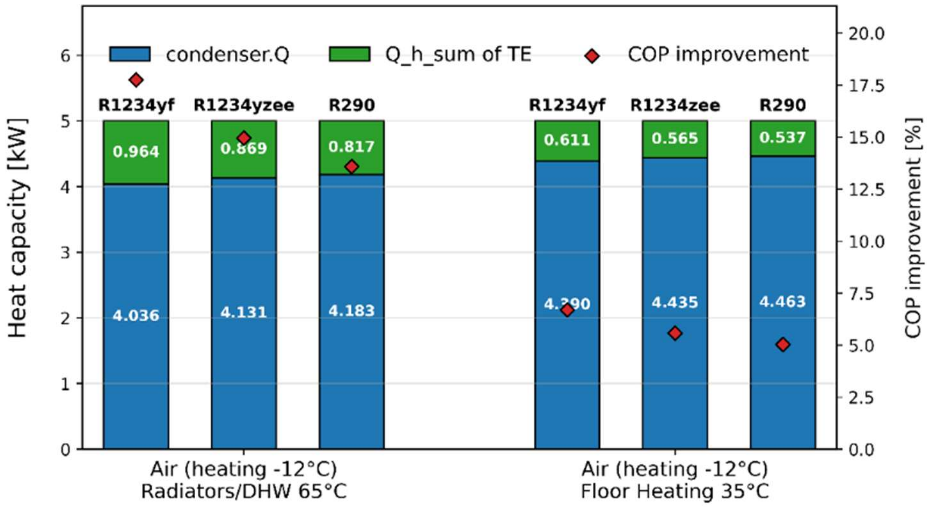

(a)

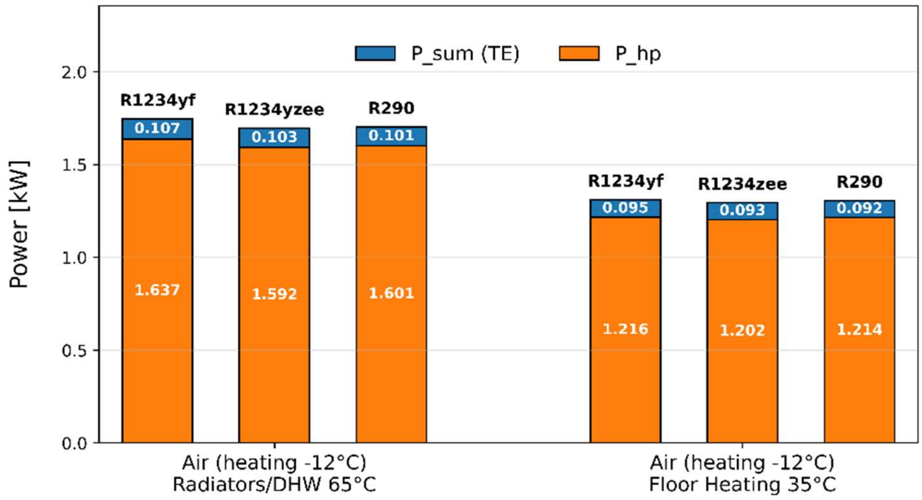

(b)

Fig. (7) HP with an active subcooler with various refrigerants, a) Heating capacity and COP improvement, b) Electrical power

Acknowledgements

The call "Technologien und Innovationen für die klimaneutrale Stadt" is part of the R&I priority "Klimaneutrale Stadt" of the Federal Ministry for Innovation, Mobility and Infrastructure (BMIMI) and the Klima- und Energiefonds (KLIEN). The programme is implemented on behalf of BMIMI and KLIEN by the Österreichische Forschungsförderungsgesellschaft (FFG) in cooperation with Austria Wirtschaftsservice Gesellschaft mbH (AWS). The authors acknowledge OTS company for providing the measurement data needed for validation of the Dymola model.

References

[1] IEA. Tracking Clean Energy Progress 2023 2023.
[2] Żelazna A, Pawłowski A. Review of the Role of Heat Pumps in Decarbonization of the Building Sector. Energies 2025;18:3255. https://doi.org/10.3390/en18133255.
[3] Hu Y, Shen B, Wan H, Gluesenkamp KR, Krishnamoorthy S, Shirey D. Heating performance of a vapor compression heat pump cascaded with a thermoelectric heat pump. Applied Thermal Engineering 2024;249:123397. https://doi.org/10.1016/j.applthermaleng.2024.123397.
[4] Konrad ME, MacDonald BD. Cold climate air source heat pumps: Industry progress and

thermodynamic analysis of market-available residential units. Renewable and Sustainable Energy Reviews 2023;188:113739. https://doi.org/10.1016/j.rser.2023.113739.
[5] Song M, Deng S, Dang C, Mao N, Wang Z. Review on improvement for air source heat pump units during frosting and defrosting. Applied Energy 2018;211:1150–70. https://doi.org/10.1016/j.apenergy.2017.12.022.
[6] European Heat Pump Association (EHPA). Financial barriers to the widespread adoption of heat pumps 2024.
[7] IEA Technology Collaboration Programme on Heat Pumping Technologies (HPT TCP). Annex 51 “Acoustic Signatures of Heat Pumps”, Final Report - Part 11 2021.
[8] Langerova E, Kralicek J, Kucera M. Air-to-water heat pump noise in residential settings: A comprehensive review. Renewable and Sustainable Energy Reviews 2025;207:114968. https://doi.org/10.1016/j.rser.2024.114968.
[9] Regulation (EU) 2024/573 of the European Parliament and of the Council of 7 February 2024 on fluorinated greenhouse gases, amending Directive (EU) 2019/1937 and repealing Regulation (EU) No 517/2014 n.d.
[10] Zhao D, Tan G. A review of thermoelectric cooling: Materials, modeling and applications. Applied Thermal Engineering 2014;66:15–24. https://doi.org/10.1016/j.applthermaleng.2014.01.074.
[11] Okuma T, Radermacher R, Hwang Y. A Novel Application of Thermoelectric Modules in an HVAC System Under Cold Climate Operation. Journal of Elec Materi 2012;41:1749–58. https://doi.org/10.1007/s11664-012-2066-x.
[12] Balasubramanian R. Overview of the use of Peltier’s modules in technology 2020.
[13] Song K, Tanvir ANM, Bappy MO, Zhang Y. New Directions for Thermoelectrics: A Roadmap from High-Throughput Materials Discovery to Advanced Device Manufacturing. Small Science 2025;5:2300359. https://doi.org/10.1002/smsc.202300359.
[14] Huang L, Zheng Y, Xing L, Hou B. Recent progress of thermoelectric applications for cooling/heating, power generation, heat flux sensor and potential prospect of their integrated applications. Thermal Science and Engineering Progress 2023;45:102064. https://doi.org/10.1016/j.tsep.2023.102064.
[15] Dongxu J, Zhongbao W, Pou J, Mazzoni S, Rajoo S, Romagnoli A. Geometry optimization of thermoelectric modules: Simulation and experimental study. Energy Conversion and Management 2019;195:236–43. https://doi.org/10.1016/j.enconman.2019.05.003.
[16] Shi L, Abed AM, Fayed M, Abdulghani ZR, Anqi AE, Khadimallah MA, et al. Economic cost analysis of air-cooling process using different numbers of Peltier modules; Experimental case study. Case Studies in Thermal Engineering 2023;41:102627. https://doi.org/10.1016/j.csite.2022.102627.
[17] Bahk J-H, Mohankumar TD, Saini A, Watzman SJ. Performance evaluation and optimization of air-to-air thermoelectric heat pump system. Energy and Buildings 2025;344:115994. https://doi.org/10.1016/j.enbuild.2025.115994.
[18] Casi Á, Aranguren P, Araiz M, Sanchez D, Cabello R, Astrain D. Performance assessment of an experimental CO 2 transcritical refrigeration plant working with a thermoelectric subcooler in combination with an internal heat exchanger. Energy Conversion and Management 2022;268:115963. https://doi.org/10.1016/j.enconman.2022.115963.
[19] Astrain D, Merino A, Catalán L, Aranguren P, Araiz M, Sánchez D, et al. Improvements in the cooling capacity and the COP of a transcritical CO2 refrigeration plant operating with a thermoelectric subcooling system. Applied Thermal Engineering 2019;155:110–22. https://doi.org/10.1016/j.applthermaleng.2019.03.123.
[20] Schoenfield J, Hwang Y, Radermacher R. CO_2 transcritical vapor compression cycle with thermoelectric subcooler. HVAC&R Research 2012;18:297–311. https://doi.org/10.1080/10789669.2012.625348.
[21] Wantha C. Experimental investigation of the influence of thermoelectric subcooler on the performance of R134a refrigeration systems. Applied Thermal Engineering 2020;180:115829. https://doi.org/10.1016/j.applthermaleng.2020.115829.